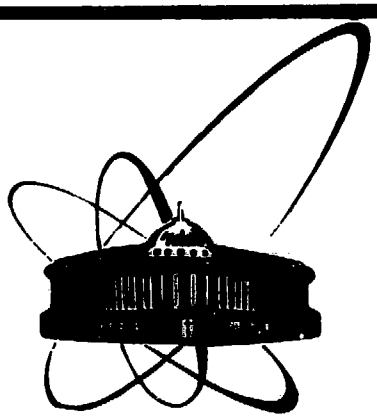

объединенный
институт
ядерных
исследований
дубна

E2-88-809

J.J.Musulmanbekov

STATISTICAL CLUSTERS IN MULTIPARTICLE PRODUCTION

Submitted to "Zeitschrift für Physik C"

1988

1. Introduction

Statistical cluster hypothesis of multiparticle production in hadronic interactions has a long time history. The reasons for this hypothesis are the following experimental facts: grouping of secondaries in rapidity space, asymmetrical events, short-range correlations and so forth. The revival of the interest to this hypothesis has been stimulated by the analysis of the multiplicity distributions of charged particles in pp and $\bar{p}p$ collisions which has been found to be well described by a negative binomial distribution at energies above 10 GeV [1]. A. Giovannini and L. Van Hove have shown that the mechanism which would give a negative binomial distribution is cluster (or clan) production one [2]. However there are many other features of multiparticle production the reproduction of which in the framework of cluster hypothesis could support such approach. They are:

1. The leading particle effect.
2. The growth of rapidity space is not nearly so rapid as a multiperipheral model gives.
3. The growth of the central rapidity density $(dn/d\eta)_{\eta = 0}$.
4. Asymmetry of a large amount of interactions.
5. Approximate KNO-scaling at the energies $\sqrt{s} \leq \sqrt{s}_{ISR}$ and it's violation at higher energies.
6. Forward-backward multiplicity correlations.
7. The growth of single-diffractive cross section at $\sqrt{s} \leq \sqrt{s}_{ISR}$ and it's approximate constancy at higher energies?
8. The growth of the average transverse momentum which enhances at collider energies.
9. The dependence of the average transverse momentum in central rapidity region on multiplicity.
10. Rising fraction with energy of "minijet" events.

Can one interpret above-mentioned features of multiparticle production on the basis of cluster hypothesis and if so,which properties do these clusters possess? An attempt to answer this question is a goal of the paper.We will construct Monte-Carlo simulation model where we use as a first approximation the bremsstrahlung analogy proposed by L.Stodolsky [3] and later developed by S.Fokorsky and L.Van Hove [4].This approach seemed to be attractive because it enables one to consider multiparticle production as fragmentation (or dissociation) of the colliding hadrons into clusters.In other words,it provides one with the uniform description of diffractive and non-diffractive processes.Throughout the construction of the model we set up some assumptions which lead to a good agreement between calculations and data. One of the key variable used in our calculations is an inelasticity which at last was an attribute of cosmic ray interactions,but at present it attracts more and more attention of collider data researchers.Inelasticity specifies a fraction of initially available energy $\sqrt{s}$,which is next found in produced secondaries.This quantity makes an analysis of multiparticle production appreciably easier.

In section 2 we start with the description of the model.In Section 3 through the comparison of the results of the model with data the assumptions and parameters for phenomenological expressions are refined.Simultaneous analysis of the model and data is made next. In Section 4 there are conclusions and discussions concerned the connection of our model with the other approaches.

2.Description of the model

Using the bremsstrahlung analogy with nucleons instead of electrons and pions instead of photons Stodolsky derived the connection between the leading particle spectrum in reaction pp—>pX and the central rapidity density of secondary pions [3]. In Ref.4 the low mass clusters are used as radiated objects yet.The basic assumptions of such approach are:

i)Leading particles and radiated pions(clusters) possess low transverse momenta.

ii)The probability of n - pions(clusters) radiated into a rapidity interval y,y+Δy follows a Poisson distribution

$$P(n) = (\rho\cdot\Delta y)^n exp(-\rho\cdot\Delta y)/n!, \qquad (1)$$

where ρ is the density of pions(clusters) in rapidity space.This is equivalent to assume that emission of clusters is statistically independent.

Now the probability that the incident particle loses the energy W is

$$P(W) = \sum \delta(W - \sum n_I w_I)\cdot \prod P(n_I), \qquad (2)$$

where the summing before δ-function is over the various configurations $n_1,n_2,\ldots$ .Substituting (1) into the right-hand side of Eq.(2) and passing from the sum to an integral Stodolsky calculated the inclusive spectrum of the leading proton

$$P(W) \longrightarrow d\sigma/dx = const\cdot(1-x)^{\rho-1}. \qquad (3)$$

To agree with the experimental spectrum he put ρ=1. However this value of particle density on rapidity space independent of energy is in contradiction with the data at higher energies ($\sqrt{s}$>10 GeV).In addition to that the model does not describe the range of the diffraction peak ($x \simeq 1$).One of the possible ways to overcome first discrepancy is to introduce the growth of cluster masses with collision energy. This is our first assumption.Second discrepancy is,in our view,a consequence of the inclusive formulation of the problem.As shown below this discrepancy is eliminated in the exclusive realization of the model.

Simulation of exclusive events is performed as follows.First,the inelasticity of the interaction or fraction of the initial c.m.energy $\sqrt{s}$ available for production of secondaries is determined.Then,using the available energy $W = K\cdot\sqrt{s}$,where K is an inelasticity,we generate clusters and their kinematics.There are four stages on which we generate inelasticity,cluster masses,cluster momenta,cluster decay.

2.1 Inelasticity

In a separate interaction inelasticity is specified as

$$K = \sum E_i \; / \; \sqrt{s}, \qquad (4)$$

where E_i is the energy of particle(cluster) i. Fluctuations of the inelasticity from event to event lead to some distribution $P(K)$.There are not elaborated theoretical methods for calculation of $P(K)$ and average inelasticity $\langle K \rangle$.Existing model calculations lead to dissimilar results.Hence we will use empirical data which paucity will be compensated by corrections derived from the comparison of results of event generation with data.The data on $P(K)$ and energy dependence of $\langle K \rangle$ for pp collisions are shown in Fig. 1 and 2.Square at $\sqrt{s}$ = 540 GeV is an estimate of Ref.2

$$\langle K \rangle_{\sqrt{s}\,=\,540\mathrm{GeV}} \; / \; \langle K \rangle_{\sqrt{s}\,=\,63\mathrm{GeV}} \simeq 0.6 . \qquad (5)$$

As was shown in Ref.10 one may fit the inelasticity distribution with a beta distribution

$$P(K,s) = K^{a-1}(1-K)^{b-1} / \; B(a,b)$$
$$B(a,b) = \Gamma(a)\Gamma(b) \; / \; \Gamma(a,b) \qquad (6)$$

with

$$\langle K(s) \rangle = a \; / \; (a+b). \qquad (7)$$

The s dependence of $P(K,s)$ and $\langle K(s) \rangle$ is contained in parameters a and b.As a result of withdrawal of K from (6) for a separate event we have the available energy W radiated clusters

$$W = K \cdot \sqrt{s} = \sum (p_i^{\,2} + M_i^{\,2})^{\,1/2}, \qquad (8)$$

where p_i and M_i are momentum and mass of cluster i.

Fig.1 Inelasticity distributions for pp collisions.Circles are compilation of data from cosmic ray experiments [7], histogram - data [8] at $\sqrt{s}$=16.5 GeV.

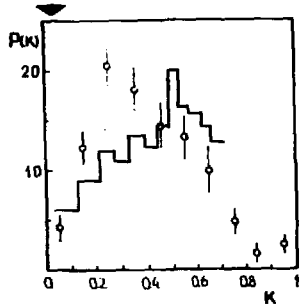

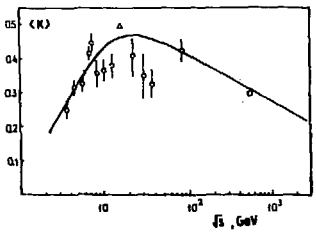

Fig.2 The average multiplicity plotted as a function of energy. Circles - compilations of the data from cosmic ray experiments [7]; triangles-data of Ref.8, square-the result of the estimation (5) from Ref.9.

Fig.3 Parameters $a - 2$ and $b - 1$ of the distribution (6) plotted as a function of energy.

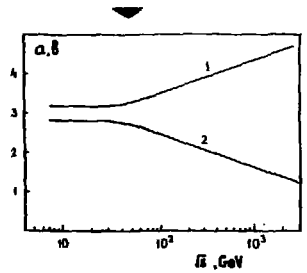

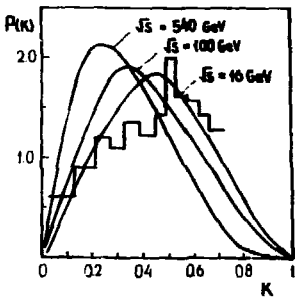

Fig.4 The inelasticity distributions at various c.m. energies. Histogram -data from Ref.8.

2.2 Cluster masses

During the collision a considerable amount of kinetic energy of colliding hadrons is converted into the excitation energy(effective mass) of emitted clusters.As with Ref.[11] cluster mass generation which is statistical in nature leads to the following distribution

$$P(M) = c \cdot M \cdot \exp(-b \cdot M). \qquad (9)$$

The parameters c and b determined by the normalization conditions

$$\int P(M) \cdot dM = 1 \qquad (10)$$

$$\int M \cdot P(M) \cdot dM = \langle M \rangle \qquad (11)$$

can be expressed in an average mass of clusters <M>. s- dependence of <M> is tuned to agree the characteristics of simulated events with data (see section 3).

The cluster mass growth with energy is necessary in our opinion by the following reasons.First to provide at least up to the top ISR energies nonvanishing contribution of single diffraction. Indeed, based on statistical nature of cluster production the less the multiplicity of produced clusters,the greater the probability of diffractive events.Cluster mass growth just restricts rapid increasing of their multiplicity with c.m.energy of colliding particles. Secondly,cluster mass growth is the one of the factors which cause the rise of central rapidity density $dn/dy_{y=0}$. Third, it provides the growth of transverse momentum of secondaries with c.m. energy.

2.3 Cluster momenta

Statistical independent emission of clusters with limited transverse momenta corresponds to a cylindrical phase space model.For cluster i the rapidity

$$y_i = \zeta_i \cdot Y_i, \qquad (12)$$

where ζ_i is random number with uniform distribution in the interval [0,1], and

$$Y_i = Y_i^{max} = 2 \cdot Ln(\sqrt{s}/(M_T)_i), \qquad (13)$$

where $(M_T)_i = [(p_T)_i^2 + M_i^2]^{1/2}$ is transverse mass of cluster i. However in this way it is difficult to obtain a consistent

description of energetic dependence of average multiplicity, rapidity distributions and single diffractive cross section. To overcome this difficulty we put forward the following assumption: the available rapidity region (ARR) for clusters depends on an inelasticity

$$Y_i = 2 \cdot \ln [\alpha(K) \cdot \sqrt{s} / (M_T)_i]. \qquad (14)$$

The phenomenological function $\alpha(K)$ is adopted as follows

$$\begin{aligned} \alpha(K) &= a_1 \cdot \exp[-(K-K_c)^2 / d_1^2], \quad K \le K_c \\ \alpha(K) &= a_2 \cdot \exp[-(K-K_c)^2 / d_2^2] + b, \quad K \ge K_c. \end{aligned} \qquad (15)$$

where $a_1 = a_2 + b$. *Such a behavior of* $\alpha(K)$ *enables one to get a* consistent description of the majority properties of multiparticle production up to ISR energies. The limitation on ARR leads to the effect that the clusters produced at inelasticities which close to 0 and 1 are concentrated essentially in the central rapidity region. At intermediate values of the inelasticity ARR increases approaching to kinematical limit Y_i^{max}. The larger ARR, the greater the probability of producing a few clusters at available energy W. Under statistical independence of a cluster emission this leads to essential fluctuations of cluster location in rapidity space in particular to asymmetry which is a distinctive feature of single diffraction. On the other hand the decreasing of ARR at the same value W leads to the decreasing of kinetic energies of clusters so the number of clusters increases. This results a more uniform cluster filling of ARR that is specific to a non-diffractive production. The parameters in expressions (15) are adjusted to get the desired features of generated events. Using a rapidity calculated from Eqs.(12) and (14), we derive energy and momentum of a cluster

$$E_i = (M_T)_i \cdot \mathrm{ch}\, y_i \qquad (16)$$

$$(p_{II})_i = (M_T)_i \cdot \mathrm{sh}\, y_i. \qquad (17)$$

The clusters are given transverse momenta from a distribution

$$f\,[(p_T)_i^{\,2}] \propto exp\,[-b\cdot(p_T)_i^{\,2}]\ . \qquad (18)$$

2.4 Leading particles

The generation of clusters is carried out till the available energy $W = K\cdot\sqrt{s}$ is not yet exhausted. The remaining part of the c.m. energy $(1-K)\cdot\sqrt{s}$ is distributed over the two leading particles which are supposed to be the main remnants of the incoming particles. The transitions taken into consideration are

$$p \longrightarrow p,n,\Delta^{++},\Delta^{+},\Delta^{0},\Delta^{-} \qquad (19)$$

$$\bar{p} \longrightarrow \bar{p},\bar{n},\bar{\Delta}^{++},\bar{\Delta}^{+},\bar{\Delta}^{0},\bar{\Delta}^{-}\ . \qquad (19')$$

For transition probabilities we use the results of OPE-model [12]. Leading particle momenta are defined by the energy-momentum conservation

$$\Sigma\, p_i = p_I + p_{II} \qquad (20)$$

$$p_I^{\,2} + m_I^{\,2} + p_{II}^{\,2} + m_{II}^{\,2} = (1-K)\cdot\sqrt{s}\ , \qquad (21)$$

where p_i is the momentum of i^{th} cluster, p_I, p_{II}, m_I, m_{II} are momenta and masses of leading particles.

In such an exclusive formulation the statistical independence of cluster emission leads occasionally to the situations when all the clusters produced find themselves within forward or backward hemisphere only. Such events are classified to be single diffractive ones and the incoming proton is supposed to fragment which remnant is in the hemisphere where the clusters produced are. The second leading particle conserves all its quantum numbers. The parameter b in Eq.(18) for the generation of transverse momenta of clusters is adjusted to get an agreement between calculated and experimental distributions for transverse momenta of a leading particle in diffractive events.

2.5 Cluster decays

In a simple case clusters can be made to decay both isotropically and following a cylindrical phase space which is adequate to a multiperipheral model. Up to ISR energies both approaches don't differ because of rather low masses of clusters. However at collider energies where cluster masses reach values of a few GeV multiperipheral decay may lead with some probability to a jet structure. A study at these energies [13] has shown that the growing part of inelastic interactions just comprises minijet events.Thus a multiperipheral decay of clusters is favored because it provides a way of describing both soft and semihard processes.Clusters are taken to be uncoloured objects possessing neutral charge for cluster masses which are more than of a pion mass. Hence we can identify them with evolving gluon-gluon and quark-antiquark pairs. We suppose that the bulk of clusters develops from quark-antiquark pairs then we derive the properties of decay particles from e^+e^--annihilation data provided $\sqrt{s}_{e^+e^-} = M_{cl}$. However it must be noted,that although annihilation processes at higher energies possess a clearly defined jet structure,mean multiplicities in them grow substantially faster than the multiperipheral model yields. Besides this,the growth of energy $\sqrt{s}_{e^+e^-}$ is accompanied by the plateau height of the rapidity distribution as well as in hadron-hadron interactions.The multiperipheral decay scheme could be agreed with this effects provided the hadronization process is performed through the production and the subsequent decay of next level clusters i.e. subclusters. However,we suppose that the detailed model treatment of cluster decay is of self-sufficient interest and therefore we use for the generation of the properties of decay particles the modified cylindrical phase space model. Modification of a model is concerned with the limitation on the logarithmic growth of rapidity,so it leads to the enhance of the dependence of an average decay multiplicity on a cluster mass.

At a rest frame of a cluster we assign to decay particle j the rapidity

$$Y_j = \xi_j \cdot Y_j = \xi_j \cdot ln\ [\ \beta \cdot M_{cl}\ /\ (M_T)_j\ ]\ , \qquad (22)$$

where ξ_j is a random number uniformly distributed in the interval [0,1], $(M_T)_j$ is the transverse mass of j^{th} particle and β depends on cluster mass

$$\beta = \beta(M) = [1+C \cdot ln(M_{cl}/\ M_0)]^{-1}\ . \qquad (23)$$

Parameters C and M_0 are adjusted in such a way that the average multiplicity of charged particles and their rapidity spectra agree with those in e^+e^- annihilation processes at $\sqrt{s}_{e^+e^-} = M_{cl}$. The particle composition is adjusted to these data too. The production of η - mesons is taken into account as a correction since they are practically lacking in annihilation processes.Transverse momenta of decay particles are drown from the following distribution:

$$f\ [(P_T)_i] \propto exp\ [-\alpha \cdot (P_T)_i^2]\ , \qquad (24)$$

assuming α = const.,i.e.it does not depend on a cluster mass. This is justified by the fact that in two jet events of e^+e^--annihilation processes average transverse momenta of hadrons depend only slightly on the energy $\sqrt{s}_{e^+e^-}$. We also assume that the direction of the decay axis of a cluster depends on its mass. The less is the cluster mass,the closer the direction of the cluster decay axis to the collision axis,and conversely if the cluster mass approaches the maximal value at a fixed collision energy,then the direction of the cluster decay axis shifts to the plane which is perpendicular to the collision axis. For simplicity we define this relationship as following

$$cos\ \vartheta = exp\ (-c \cdot M\ /\langle M \rangle)\ , \qquad (25)$$

where ϑ is the angle between decay axis and collision axis, c is a parameter and $\langle M \rangle$ is the average mass of clusters.

3. Comparison of generated events and data

3.1 Parameter adjustment and single diffractive cross section

The energetic dependence of the inelasticity distribution $P(K,s)$ and its mean value $\langle K(s)\rangle$ manifest through the values of free parameters a and b in Eqs.(6) and (7).Because of the uncertainty of experimental data there exist some arbitrariness in choosing these parameter values. We refine them by comparing those features of calculated and experimental events which are sensitive to the form of the distribution $P(K,s)$.The best suited values of parameters a and b are shown in Fig.3. Such a behavior of these parameters corresponds to the average inelasticity calculated by Eq.7 to be equal 0.45 for $\sqrt{s} \leq$ 15–30 GeV and to decrease at higher energies (Fig.2).The actual decreasing of $\langle K(s)\rangle$ at $\sqrt{s} \leq$ 15 GeV which is in agreement with data is due to the kinematical limit $W < \sqrt{s}-m_I'-m_{II}'$ i.e., the masses of remnants I and II are comparable to the total c.m.energy. The calculated inelasticity distributions are shown in Fig.4. As can be seen,the maxima of the distributions shift with the energy growth to the range which corresponds to the smaller values of K and this shift is accompanied by the narrowing of the distributions

Parameterizations being used to generate cluster masses are adjusted from the comparison between the results of calculation and the data.To get a good description of single diffractive (SD) and non-single diffractive (NSD) interactions up to ISR energies one can use a logarithmic dependence of cluster mass on energy

$$\langle M\rangle = a + b\cdot ln(\sqrt{s}/\sqrt{s_0}), \qquad (26)$$

where a = 0.10 GeV, b = 0.25 GeV, s_0= 1 GeV (Fig.5). In doing so the parameters for $\alpha(K)$ in (15) are K_c=0.33, a_1= 0.75, a_2= 0.45, d_1=0.025, d_2= 0.065, b= 0.30.

However,at higher energies ($\sqrt{s} > \sqrt{s}_{ISR}$) the calculated average multiplicity of charged particles increases considerably slower than the experimental one does (dashed curve in Fig.6).To avoid this disagreement one may use the following ways:

i) To enhance the energetic dependence of cluster masses.

ii) To reduce the maximum of $\alpha(K)$ with energy growth.

iii) To combine both methods i and ii.

Although the first method makes it possible to have a correct energetic dependence of the average multiplicity of charged particles it leads to discrepancy between predicted and experimental rapidity distributions:the central rapidity density increases more rapidly than that in the experiment. The similar effect must be evident in three-fireball model (TFM) [11],in which the constant number of the clusters (fireballs) independent on collision energy is provided by the rapid increasing of their masses.

Using method ii only ,we are faced with difficulties in reproducing transverse momenta and a fraction of minijet events. So we use the combination of both methods. We shall define the energetic dependence of the cluster mass as

$$\langle M \rangle = 0.30 + 0.12 \cdot s^{1/4} \ . \qquad (27)$$

At the energies $\sqrt{s} \leq \sqrt{s}_{ISR}$ this dependence agrees very closely with a logarithmic curve (26) (Fig.5).

Curves for $\alpha(K,s)$ at different energies are shown in Fig.7 a. Energetic dependence of $\alpha(K,s)$ amounts to the decreasing of parameters a_1,a_2 and b in (15). As it follows from (14),the cluster mass growth and the reducing α_{max} moderate the logarithmic growth of rapidity space. Reducing α_{max} with the energy growth shifts the spectrum of produced clusters $d\sigma/dx$ to smaller x. In quark-parton models the similar shift of produced particles spectra results from the increasing contribution of the gluonic component or the extra strings formed by sea quark-antiquark pairs. It should be noted that the maximum rate of reduction of α_{max} occurs at energy range $\sqrt{s} \simeq 50 - 200$ GeV (Fig.8).

Thus it is possible to agree the calculations and data for average multiplicities (solid curve in Fig.6),rapidity distributions and transverse momenta at a whole accelerator energies provided one introduces a more strong dependence of cluster masses on energy and the evolution of $\alpha(K,s)$. However in doing so one reveals two essential discrepancy between the results of

Fig.5 The energetic dependence of the average mass of clusters. Dashed curve corresponds to formula (26), solid curve-to formula (27).

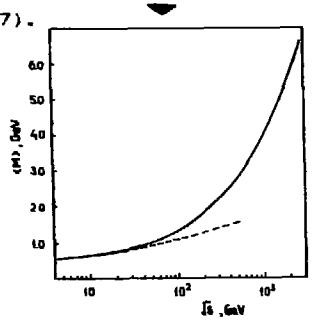

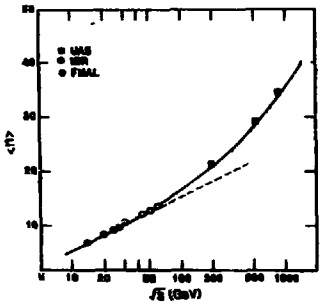

Fig.6 The energetic dependence of the average multiplicity of charged particles. Explanations are in the text.

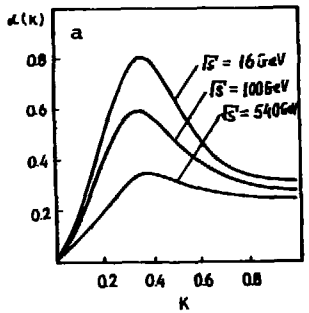

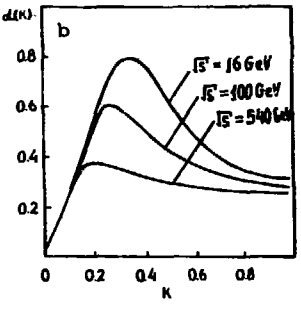

Fig.7 Phenomenological function $\alpha(K,s)$ (Eqs.15) at various energies. *a*)The position of α_{max} in inelasticity space does not change; *b*)the position of α_{max} is defined by Eq.28.

calculation and data. On the one hand,the calculated multiplicity distributions at energies $\sqrt{s} > \sqrt{s}_{ISR}$ trend to narrow,whereas the data exhibit the opposite behavior. On the other hand, calculated single diffractive cross section σ_{SD}* first attains a maximum at

* $\sigma_{SD}=(N_{SD}/N_{in})\cdot\sigma_{in}$,where N_{SD}- the number of SD events, N_{in}- the total number of inelastic interactions, σ_{in}-the experimental value of the inelastic cross section.

top ISR energies,then trends to decrease more and more deviating from the data [14] (Fig.9). To refine the agreement between calculated and experimental values of σ_{SD} one has to enhance a fraction of coherent processes at smaller inelasticities. To do this the reduction of α_{max} must be supplemented by a shift of its position K_c to lesser values of inelasticity. Since the average inelasticity decreases with the energy growth,we shall express the energetic dependence of the position of maximum K_c in the form

$$K_c = \gamma \cdot \langle K(s) \rangle^{\beta}, \qquad (28)$$

where $\gamma = 0.65$, $\beta \simeq 1$. Adjusted in such a way a function $\alpha(K,s)$ is shown at different energies in Fig.7 b. SD cross sections obtained by using the corrections mentioned above are shown in Fig.9. The dispersion of calculated values of σ_{SD} is due to certain arbitrariness in choosing parameters for $\alpha(K,s)$, which are also fixed by an agreement between the calculated multiplicity distributions and the experimental ones. A detailed analysis of multiplicity distributions is performed below. Note that the shift of the position of $\alpha_{max} = \alpha(K_c)$ with the energy growth causes the appearance of minimum in the energetic dependence of σ_{SD} at $\sqrt{s} \simeq$ 200 GeV. Almost all models [15-18] predict a monotonic behavior of $\sigma_{SD}(s)$ in the energy range $\sqrt{s} > \sqrt{s}_{ISR}$. Hence, in our opinion, it is of great interest to take a comprehensive measurements of SD cross sections σ_{SD} in energetic interval $\sqrt{s}_{ISR} < \sqrt{s} < \sqrt{s}_{SPS}$.

3.2 Multiplicity distributions

As was revealed at the energies $\sqrt{s} \leq \sqrt{s}_{ISR}$, multiplicity distributions of charged particles depicted in the form $\psi(z)=\langle n \rangle \cdot P_n$, where $z = n/\langle n \rangle$,do not depend on the energy of colliding baryons (KNO - scaling) [19]. However data analysis at collider energies exhibited deviations from this law: the higher c.m.energy,the larger the fraction of events with $z \geq 2$ [20]. Dynamical and statistical aspects of scaling behavior of multiplicity distributions are the subject of much theoretical investigations.

In our approach the energetic dependence of inelasticity distributions and $\alpha(K,s)$ play an important role in multiplicity distributions behavior. Let us express the multiplicity distributions $P_n(s)$ in the conditional multiplicity distributions $P(n|K)$

$$P_n(s) = \int P(K,s) \cdot P(n|K) \cdot dK . \qquad (29)$$

Fig.8 α_{max} plotted as a function of energy.

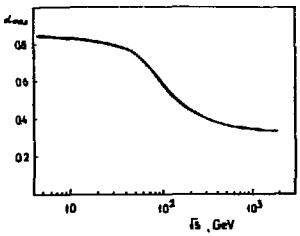

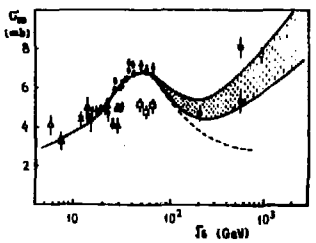

Fig.9 The energetic dependence of σ_{SD}. Data compilation is from Ref.14. Curves - our calculations.Explanations are in text.

Fig.10 The multiplicity distributions of charged particles in pp collisions plotted in KNO-form at inelasticities *0.4-0.5*. Points - data of Ref.21. Dashed curve is our calculations; solid curve - the best fit of data for total inelastic events [21].

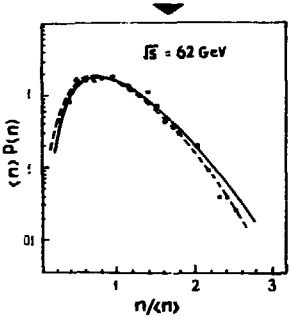

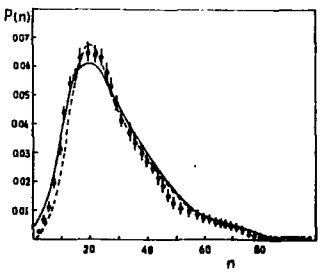

Fig.11 The multiplicity distributions of charged particles in $\bar{p}p$ collisions at $\sqrt{s}$ = 540 GeV/

Here we treat variable n as a multiplicity of clusters, that is we assume that the behavior of multiplicity distributions of charged particles is defined by the behavior of the multiplicity distributions of clusters. This is justified by the fact that cluster decay spectra are considerably narrower than $P_n(s)$. An exact scaling of distributions (29) would occur in the case of energetic independence of inelasticity distributions $P(K,s)$ and of scaling behaviour of distributions $P(n|K)$. The features of distributions $P(n|K)$ depend on the behaviour of $\alpha(K,s)$, and if it does not change with energy, then the distributions $P(n|K)$ would be described by a uniform scaling function at a fixed inelasticity K. With scaling of $P(K,s)$ this would lead to scaling of the total distribution $P_n(s)$. This situation holds approximately up to ISR energies, that is the distributions $P_n(s)$ take the scaling form. What is more the multiplicity distributions $P(n|K)$ at $\sqrt{s}$ = 62 GeV in inelasticity interval 0.2-0.5 can be depicted by $\psi(z)$-function which is close to the scaling function for the total distributions $P_n(s)$. Such similarity of the distributions $P_n(s)$ and $P(n|K)$ in KNO-form is due to two reasons. First, this interval corresponds to a range of maximum of inelasticity distributions $P(K,s)$. Secondly, the values of $\alpha(K,s)$ in this interval are nearly to 1 and in consequence the distributions $P(n|K)$ possess the greatest possible dispersions.

The reduction of a maximum of $\alpha(K,s)$ at $\sqrt{s} > \sqrt{s}_{ISR}$ (Fig.7a) causes the shift of distributions $P(n|K)$ towards large multiplicities which is followed by the narrowing of the distributions. In its turn the narrowing of the distributions $P(n|K)$ leads to the situation when the shape of the distributions $P_n(s)$ is increasingly dictated by the shape of inelasticity distribution at corresponding energy (Fig.4). This connection manifests itself in the relative narrowing of the distributions $P_n(s)$ and the occurrence of a long tail at high multiplicities while c.m.energy increases (dashed curve in Fig.11). Introduced to reproduce SD-cross sections the shift of the position of α_{max} in K-space (Fig 7b) leads to the increasing of dispersions of the distributions $P(n|K)$ at small inelasticities that, in turn, markedly violates the similarity between $P(K,s)$ and $P_n(s)$ (solid curve in Fig.11). Eventually, this results in the widening of $P_n(s)$ and not

Fig.12 γ_2-moments of multiplicity distributions plotted as a function of energy. Data from Refs.22 and 23. Dashed curve is a calculation without a shift of the position of α_{max} in inelasticity space; solid curve -that with a shift (28).

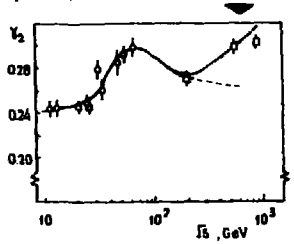

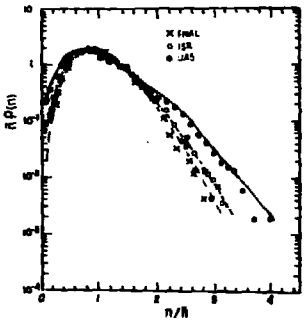

Fig.13 The multiplicity distributions of charged particles plotted in KNO-form. Data-from Refs.22 and 23.

Fig,14 The average cluster multiplicity plotted as a function of energy. Circles-results of calculation from Ref 2 and 24.

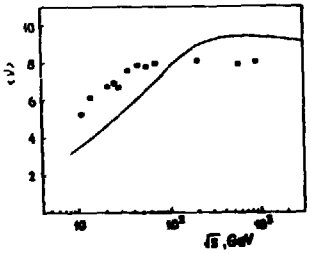

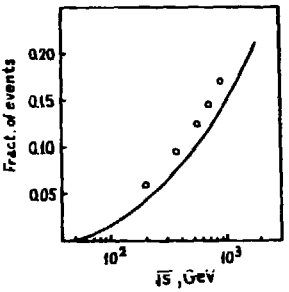

Fig.15 The fraction of jet events with $E_T^{jet} > 5$ GeV in pseudorapidity range $|\eta| < 1.5$. Circles - data from Ref.13.

only for total inelastic interactions but also for NSD ones. One can say that the shape of multiplicity distributions for NSD events $\sqrt{s} > \sqrt{s}_{ISR}$ is connected with the contribution of diffractive events. Fig.12 shows the energetic dependence of γ_2-moments of the distributions $P_n(s)$ for NSD-events. When comparing it with

energetic dependence of SD-cross sections σ_{SD} (Fig.10), one notes that they are similar.

How the calculated multiplicity distributions agree with data [22,23] one can judge from Fig.13.

3.3 Average number of (super)clusters

Analysis of multiplicity distributions of charged particles in the framework of the cluster mechanism revealed that the average number of produced clusters $\langle\nu\rangle$ increases with energy achieving a saturation at $\sqrt{s} \geq 60$ GeV (Fig.14).

We have also obtained the similar growth of $\langle\nu\rangle$ with energy although the energy of saturation in our approach is somewhat higher. The behaviour of the average number of clusters depends on three factors: the available energy $\langle M\rangle=\langle K(s)\rangle\cdot\sqrt{s}$, cluster masses M_i, and the shape of $\alpha(K,s)$. The growth of $\sqrt{s}$ and the reduction of α_{max} promote the increasing of $\langle\nu\rangle$; but the increasing of $\langle M(s)\rangle$ and the decreasing of $\langle K(s)\rangle$ - the decreasing of $\langle\nu\rangle$. The saturation of $\langle\nu\rangle$ at collider energies is a result of competition of these two trends. If a tendency for the decreasing of $\langle K\rangle$ is preserved, then the value of $\langle\nu\rangle$ at $\sqrt{s} > \sqrt{s}_{ISR}$ would begin decreasing.

The difference between the maximum values of $\langle\nu\rangle$ obtained in our approach and by the authors of papers [2,24] stems, in our opinion, from the fact that in [2,24] they didn't take into account the production of neutral particles.

3.4 Minijets

It has been observed by UA1 Collaboration [13] that the increasing fraction of minimum bias events with energy growth is made up from so-called "minijet" events. Such events were found when they measured the charge multiplicity distributions and transverse energy E_T distributions in the rapidity region $|\eta|<2.5$ under the condition that at least 5 GeV should enter the trigger cone of radius $R=[(\Delta\phi)^2+(\Delta\eta)^2]^{1/2}=1$ in the $\phi-\eta$ space (ϕ-azimuthal angle, η-pseudorapidity). The minijet events have the following striking features:

A. Their average multiplicity is approximately twice as high as that in non-minijet events.

B. The multiplicity distributions of the minijet events when plotted in KNO-form is much narrower than the corresponding curve for minimum bias events.

Formation of such jets in our approach is a natural consequence of the following assumptions of the model:

i) The increasing of cluster masses with energy.

ii) Similarity of cluster decay spectra to those in hadroproduction processes of e^+e^--annihilation.

iii) The dependence of the angle between cluster decay axis and collision axis in a relative mass of clusters (25).

As shown in Fig.15, the model yields somewhat less fraction of minijet events than experiments. The possible reason of this discrepancy is the lack of the dependence of cluster mass on the inelasticity, i.e., essentially higher mass clusters are generated in central collisions than those in peripheral collisions. However, our calculations reproduce well the features A and B.

3.5 *Average transverse momentum*

The transverse momenta of secondaries in our approach are formed from

i) Transverse momenta of clusters and directly produced particles.

ii) Transverse momenta of the decay particles in c.m. frame of a cluster.

iii) Transverse momenta of jets which are caused by deviations of the directions of the cluster decay axis from the collision axis.

At the energies $\sqrt{s} < \sqrt{s}_{ISR}$ where the main contribution to the multiparticle production is given by direct hadrons and low mass clusters, transverse momenta of secondaries is defined by factors a and b. Succeeding growth of the collision energy is characterized by the rapid growth of cluster masses, the decay of which may lead to the production of jets. Thus the changing of the energy dependence regime of $\langle P_T \rangle$ at $\sqrt{s} > \sqrt{s}_{ISR}$ (Fig.16) is the result of the rapid growth of cluster masses.

Fig.16 $\langle P_T \rangle$ for charged particles plotted as a function of energy. Points - data from Refs.26 and 27.

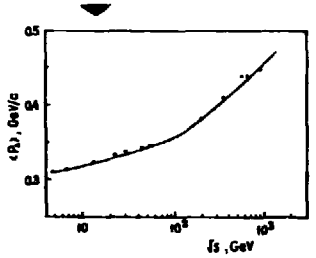

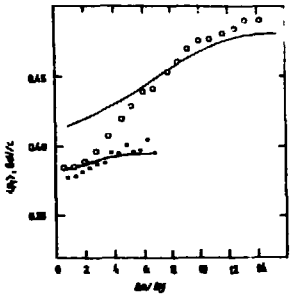

Fig.17. $\langle P_T \rangle$ for charged particles as a function of $dn/d\eta$, the density of charged particles per unit of pseudorapidity in the region $|\eta|<2.5$. Circles - data from Ref.27 at $\sqrt{s}$=540 GeV, points - from Ref.28 at $\sqrt{s}$=63 GeV.

Fig.18 Rapidity and pseudorapidity distributions (dashed and solid curves) for NSD events at $\sqrt{s}$=540 GeV.

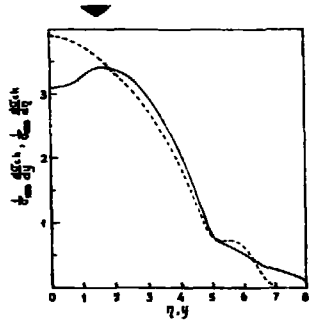

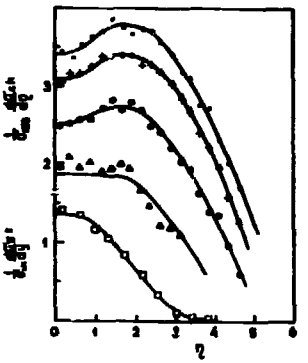

Fig.19 Pseudorapidity distributions for NSD events at various c.m. energies: Δ -53, O -200. + -540, • -900 GeV from Ref.30; □ $-E_L$= 200 GeV from Ref.31.

Collaboration UA1 [27] has observed that there are essential correlations between $\langle P_T \rangle$ for secondaries in the central rapidity region and their multiplicities (Fig.17). At $\sqrt{s}$ = 540 GeV there is a continued increase of $\langle P_T \rangle$ with the rapidity density dn/dy up to

about $dn/dy \simeq 10$ particles per unit of rapidity in the region $|y|<2.5$. Similar but more weak variations of $\langle P_T \rangle$ have been observed at ISR energies [28]. Fig.17 shows that the calculations result in a somewhat less slope of the curves than the experimental ones. The possible reason of this distinction is connected with the neglecting in our model of the dependence of cluster masses on inelasticity.

3.6 Rapidity distribution

Usually at high energies one uses in analysis of data a pseudorapidity

$$\eta = - \ln [tg(\theta/2)], \qquad (30)$$

instead of a rapidity

$$y = 0.5 \cdot \ln[(E+P_{II})/(E-P_{II})] \qquad (31)$$

assuming the equivalence of these notions. However, as shown in paper [29], this equivalence takes place for $m/P_T \geq 1$. Fig.18 shows the calculated rapidity and pseudorapidity distributions for charged particles for NSD--events at $\sqrt{s}$=540 GeV. One can see that they differ particularly in central region. Fig.19 illustrates a good agreement between calculated and experimental pseudorapidity distributions. The central pseudorapidity density growth arises in our approach from the increasing of cluster masses and the evolution of function $\alpha(K)$.

3.7 Leading baryon spectra

At FNAL and ISR energies, as has been shown in papers [32], the inclusive spectrum of protons $d\sigma/dx$ in reaction pp-->pX presents a uniform distribution except a diffractive peak region (Fig.20). From the point of view of bremsstrahlung analogy [3] such spectrum is the case if the rapidity density of produced particles ρ equals about 1 (see Eq.(3)) and does not depend on the collision energy. But, as is seen from data, ρ increases in this energy range that seemingly contradicts to Stodolsky's approach. If we will consider ρ as a density of produced clusters ρ_{cl} with masses

increasing with energy, this contradiction is removed since the value of ρ_{cl} slightly depends on c.m.energy and is near to 1 up the collider energies. However the shape of the leading baryon spectrum gradually changes with energy growth: the uniform distribution is deformed, so the distribution weight shifts to larger values of x (Fig.20). Such a behavior of the spectrum $d\sigma/dx$ is a consequence of the evolution of the inelasticity distributions and of a function $\alpha(K,s)$. Indeed, imagine the multiparticle production process which is free from fluctuations of kinematical properties of secondaries (clusters) emitted in forward and backward directions in c.m.frame. A similar situation takes place if a multiparticle production results from the formation of the central fireball with zero momentum in c.m.frame of colliding particles. Then the leading baryon spectrum $P(x,s)$ is just the inversion of the inelasticity distribution $P(K,s)$ about point $K=0.5$ because of $x=1-K$. At ISR energies inelasticity distributions have a maximum at $K\cong 0.4$ (Fig.5) and the symmetrical about $K=0.5$ distribution $P(x,s)$ has it at $x\cong 0.6$. Fluctuations of kinematical properties of secondaries, which occur actually, is in our approach essentially the consequence of statistical character of cluster emission and these fluctuations are the greater, the closer ARR to the kinematical limit (13). At the energies $\sqrt{s} \leq \sqrt{s}_{ISR}$ this is the case for the main part of events because the values of $\alpha(K,s)$ are nearly unit at the inelasticity region $0.2-0.6$ (Fig.7). The momentum conservation law (20) leads to that these fluctuations dilute the shape of the distributions $P(x,s)$ up to the experimentally observed uniform spectrum $d\sigma/dx$. At collider energies these fluctuations are essentially less hence the dilution extent of the distributions $P(x,s)$ is not so significant as it was at ISR energies.

3.8 Forward-backward multiplicity correlations

It has been observed [33-35] that there is a correlation between multiplicities of charged particles in forward (F) and backward (B) hemispheres. Fig.21 shows the dependence of the average multiplicity in backward hemisphere $\langle n_B \rangle$ in the pseudorapidity interval $-4<\eta<-1$ on the multiplicity in the forward hemisphere in

Fig.20 Inclusive spectrum for protons from reaction pp-->pX at ISR energies.Points - data from Ref.32.Curves - our calculations;dashed curve - inclusive spectrum for leading particles in reaction $\bar{p}p$-->$\bar{p}X$ at $\sqrt{s}$=540 GeV.

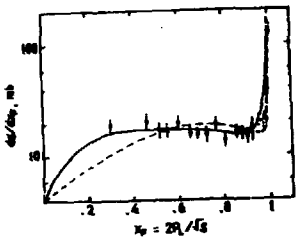

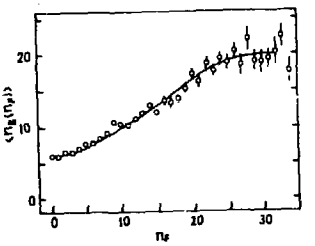

Fig.21 Dependence of the average multiplicity of charged particles in backward hemisphere in the pseudorapidity interval $-4<\eta<-1$ on the multiplicity in forward hemisphere in the interval $1<\eta<4$. Circles - data from Ref.34.

Fig.22 Energetic dependence of the strength of the forward-backward correlations. Data from Refs. 33-35.

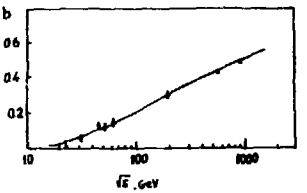

the symmetrical interval $1<\eta<4$ at $\sqrt{s}$ =540 GeV. This dependence can be approximated by a linear function

$$\langle n_B(n_F)\rangle = a + b\cdot n_F \ , \qquad (32)$$

where the parameter b,characterizing a strength of correlation, equals about 0.45. Such correlations are long range ones in contrast to short range correlations which are the result of decay of low mass clusters and resonances. Similar correlations occur at ISR energies also,although the value of parameter b is appreciably less that is the long range correlations increase (Fig.22). As can be seen in Fig.21 our model well describes a long range correlations. It must be noted however that a linear approximation is a crude approximation. The calculated curve $\langle n_B(n_F)\rangle$ is characterized by a more weak slope at small and large values of n_F than that at intermediate values. In a framework of our model these correlations are in general a result of increasing of the

cluster density ρ_{cl} in rapidity space. In turn ρ_{cl} depends on an inelasticity of interaction and ARR. The greater the inelasticity, the higher ρ_{cl} with the simultaneous increasing of n_F that leads eventually to the dependence of $\langle n_B \rangle$ on n_F.

In hadroproduction processes in e^+e^--annihilation long rang correlations are practically absent or at least very weak [36]. From our point of view, this is a case because the inelasticity in these processes is fixed (equal unit).

Let us clarify why the calculated dependence $\langle n_B(n_F) \rangle$ deviates from a linear approximation (32). A weakening of the dependence $\langle n_B(n_F) \rangle$ at large values of n_F takes place because the inelasticity for these n_F does not practically change and is close to its maximum value. Weakening of the correlations at small values of n_F is because of that the value of ARR corresponding to inelasticities realized at these n_F is maximum at collider energies. The larger the values of $\alpha(K,s)$ (Fig.7b), the larger ARR, and the less the cluster density in ARR that means the growth of fluctuations of cluster multiplicities in forward and backward hemispheres. And at large fluctuations the impact of the inelasticity on the features of produced particles is weakened.

These fluctuations are the main reason of weakening of long range correlations at lower energies, since the values of $\alpha(K,s)$ become close to unit for the bulk of interactions.

4. Discussions and summary

We have positively answered the question about the possibility of the description of the multiparticle production in the framework of the cluster mechanism and have derived the properties of these clusters. They are the following:

A. The cluster masses grow with the energy according to (27) and this growth enhances at the energy range $\sqrt{s} > \sqrt{s}_{ISR}$.

B. The average cluster multiplicity $\langle \nu \rangle$ increases up to energies $\sqrt{s} \simeq 300$–400 GeV and then starts slightly to decrease. The maximum value of $\langle \nu \rangle$ is about 10.

C. The decay of a cluster of mass $M_{cl} \gg m_\pi$ is similar to hadroproduction process in e^+e^--annihilation. The low mass clusters are suggested to be pions and mesonic resonances.

Although our model is semiempirical it is a self-consistent one since it gives a complete description of multiparticle production for SD events as well as for NSD events. Self-consistence of the model enables us to make certain predictions in those regions of the collision energy where data are absent or contain essential statistical and systematical errors. For example, the data on SD cross sections (Fig.9) cannot be fitted by a unique energetic dependence, as the calculations show for σ_{SD} the minimum at the energies about 200 GeV.

The changing of the multiparticle production regime at the energies $\sqrt{s} > \sqrt{s}_{ISR}$ (KNO-scaling violations, a rapid growth of $\langle p_T \rangle$, minijet production) is governed in the model by a rapid growth of cluster masses and the evolution of $\alpha(K,s)$ and the inelasticity distributions. These features of the model may be related to the properties of the famous models and approaches. For example, in dual parton model (DPM) [37] the leading diagram involves two strings stretched between valence quarks and diquarks of colliding baryons. Obviously, the intermediate objects which develop in the result of these string breaking correspond to our clusters. As the collision energy increases the contribution of extra strings arisen from the sea quarks and their effective masses $(M=(x_1 \cdot x_2 \cdot s)^{1/2})$ increase. The analogy to this effect in our approach is the reduction of α_{max} with the energy growth, that causes the concentration of clusters in central rapidity range.

The evolution of the inelasticity distributions can be associated with the evolution of the inelastic overlap function in impact parameter representation [38]. Analyzing the inelastic overlap function *, Henzi and Valin [39] have shown that the increasing of the inelastic cross section $\sigma_{in}(s)$ from 53 to 540 GeV is due particularly to the enhancement of the absorption at impact parameters which are close to about 1 fm. Clearly, this leads to the growth of the effective radius of inelastic interactions. Although the connection between impact parameter and inelasticity is not unique, it would be intuitively apparent that the larger the impact parameter value, the less the inelasticity. Taking into account the

* To define the inelastic overlap function $G(b,s)$, it can be used the expression for the inelastic cross section $\sigma_{in}(s) = \int d^2b \cdot G(b,s)$.

fact that the geometrical scaling [40] violates, one can suggest that the evolution of inelasticity distributions and the decreasing of $\langle K \rangle$ are due to more peripheral inelastic collisions.

As shown above cluster masses begin to increase with the collision energy particularly at $\sqrt{s} > \sqrt{s}_{ISR}$.How to agree this effect with the results of the correlation analysis which says that the multiparticle production in pp and $\bar{p}p$ collisions at the energy range ISR-SPS results from the production of small size(low mass) clusters, which then decay in average into about 2 charged particles?In order to agree these two approaches, we assume that the decay of our (super)cluster is a branching process and the small size clusters are produced at the final stage of this process. The whys and wherefores of our assumption follow from the similarity between the decay of our (super)clusters and the hadroproduction processes in e^+e^- -annihilation because the latter is well described by branching models [41,42].

Collaboration UA5 [43] has developed the program GENCL generating pp inelastic interactions, in which a multiparticle production is shared into two stages. First, low mass clusters are produced and then these clusters decay into final hadrons. Although GENCL describes a bulk of features of multiparticle production which are not fed into the program, there are some discrepancies between its results and data. As example of such discrepancies are forward-backward correlations which, in our opinion, are sensitive to the choice of the initial cluster size. At the optimal cluster size (clusters decay in average into about 1.8 charged particles) corresponding to the consistent description of the data,GENCL overestimates the correlation strength. As shown in previous section forward-backward correlations are weakened by the fluctuations of cluster distribution in ARR. The larger the size of clusters, the less the density of clusters in ARR, that leads to larger fluctuations of their distribution in rapidity space.

Thus our approach, in which the size of (super)clusters increases,is favored. Again an explicit manifestation of superclusters are, in our view, minijets.

I am indebted to my colleagues in LCTA for fruitful discussions.

References

1.UA5 Collaboration ,G.F.Alner et al., Phys.Lett.,1985,v.B160,p.199.

2.A.Giovannini and L.Van Hove, Z.Phys.,C-Particles and Fields, 1986,v.30,p.391.

3.L.Stodolsky, Phys.Rev.Lett.,1972,v.28,p.60.

4.S.Pokorsky and L.Van Hove, Acta Phys.Pol.,1974,v.B5,p.229; Nucl.Phys.,1975,v.B86,p.243.

5.M.Basile et al., Phys.Lett.,1981,v.B99,p.247; Lett.Nuovo Cim., 1984,v.41,p.229.

6.G.N.Fowler,R.M.Weiner and G.Wilk, Phys.Rev.Lett.,1985,v.55,p.173.

7.V.S.Barashenkov,N.B.Slavin, Acta Phys.Pol.,1981,v.B12,p.563.

8.D.Brick et al., Phys.Lett.,1981,v.B103,p.242.

9.R.Weiner,in:Hadronic Matter under Extreme Conditions,1986,Kiev, Naukova Dumka,p.261.

10.G.N.Fowler et al., Phys.Lett.,1984,v.B145,p.407.

11.Chou Kuang-chao,Liu Lian-sou and Meng Ta-chung,Phys.Rev., 1983,v.D28,p.1080; Cai Xu,Liu Lian-sou and Meng Ta-Chung, Phys.Rev., 1984,v.D29,p.869.

12.K.G.Boreskov,A.A.Grigorian,A.B.Kaidalov, Yad.Fiz.,1976,v.24, p.789.

13.F.Gerardini, Proc.Int.Europhys.Conf.on High Energy Physics, Bari,1985,p.363.

14.R.E.Ansorge et al., Z.Phys.C-Particles and Fields, 1986,v.33,p.175 and reference there in.

15.R.G.Roberts and D.P.Roy, Nucl.Phys.,1977,v.B77,p.240.

16.A.B.Kaidalov,K.A.Ter-Martirosyan, Phys.Lett.,1982,v.B117,p.246.

17.A.Donnachie,P.V.Landshoff, Nucl.Phys.,1984,v.B224,p.322.

18.L.Van Hove,K.Fialkowski, Nucl.Phys.,1976,v.B107,p.211.

19.Z.Koba,H.B.Nielsen and P.Olesen, Nucl.Phys.,1970,v.B40,p.317.

20.B.R.Ward in Proc.of the 3rd Topical Workshop on Proton-Antiproton Collider Physics,Roma,1983.

21.M.Basile et al., Lett.Nuovo Cim.,1984,v.41,p.293.

22.UA5 Collaboration,K.Alpgard et al., Phys.Lett.,1983,v.B121,p.209; G.Alner et al., Phys.Lett.,1984,v.B138,p.304; Phys.Lett.,1985, v.B160,p.193.

23.W.Tome et al., Nucl.Phys.,1972,v.B129,p.365; J.Firestone et al., Phys.Rev.,1976,v.D14,p.2902.
24.G.Ekspong, Proc.of XVI-th Multip.Dyn.Symp.,1985,France.
25.V.Simak,M.Sumbera and I.Zborovsky, in:Proc.of the IX-th Warsaw Symp.on Elem.Part.Phys.,1986.
26.A.M.Rossi et al., Nucl.Phys.,1975,v.B84,p.269.
27.G.Arnison et al., Phys.Lett.,1982,v.B118,p.167.
28.A.Breakstone et al., in:Proc.of High Energy Phys.Confer.,1983, Brighton.
29.Per Carlson,in;Proc.of XI-th Int.Winter Meet.on Fund.Phys.,1983, Toledo.
30.UA5 Collaboration,G.J.Alner et al., Zeit.Phys.C-Particles and Fields,1986,v.33,p.1.
31.T.Kafka et al., Phys.Rev.,1977,v.D16,p.1261.
32.J.W.Chapman et al., Phys.Rev.Lett.,1974,v.32,p.257; P.Capilluppi et al., Nucl.Phys.,1974,v.B70,p.1.
33.S.Uhlig et al., Nucl.Phys.,1978,v.B132,p.15.
34.UA5 Collaboration,K.Alogard et al., Phys.Lett.,1983,v.B123,p.361.
35.UA5 Collaboration,B.Holl,in:Proc.of the Int.Europ.Conf.on High Energy Phys.,1987,Uppsala.
36.M.Derrick et al., Zeit.Phys.C-Particles and Fields,1988,v.35, p.323.
37.A.Capella,A.Staar and J.Tran Thanh Van, Phys.Rev..,1985,v.D32, p.2933.
38.R.Henzi and P.Valin, Phys.Lett.,1974,v.B48,p.115.
39.R.Henzi and P.Valin. Phys.Lett.,1983,v.B132,p.443.
40.J.Diaz de Deus, Nucl.Phys.,1973,v.B59,p.231.
41.T.D.Gottschelk, Nucl.Phys.,1984,v.B239,p.349.
42.B.R.Webber, Nucl.Phys.,1984,v.B238,p.492.
43.UA5 Collaboration, G.J.Alner et al., Nucl.Phys.,1987,v.B291, p.445.

Received by Publishing Department
on November 18, 1988.

Мусульманбеков Ж.Ж. E2-88-809

Статистические кластеры в процессах множественного рождения частиц

Рассматривается возможность детального описания характеристик множественного рождения в дифракционных и недифракционных процессах в pp- и $\bar{p}p$-столкновениях при высоких энергиях с использованием гипотезы статистического испускания кластеров. Такое описание становится возможным при следующих основных предположениях: 1) массы кластеров растут с энергией столкновения; 2) быстротный интервал, заселяемый кластерами, зависит от неупругости и энергии столкновения; 3) распад кластеров с массами $M_{cl} \gg m_\pi$ идентичен процессу адронизации в e^+e^--аннигиляции. Создана программа генерации эксклюзивных событий. Показано, что в интервале энергий $\sqrt{s} \simeq 50$–200 ГэВ происходит изменение поведения сечения однократной дифракции.

Работа выполнена в Лаборатории вычислительной техники и автоматизации ОИЯИ.

Препринт Объединенного института ядерных исследований. Дубна 1988

Musulmanbekov J.J. E2-88-809

Statistical Clusters in Multiparticle Production

The possibility of describing multiparticle production in single-diffractive and non-single-diffractive interactions for pp and $\bar{p}p$ collisions is treated using the hypothesis of statistical cluster emission. The description is valid under the following basic assumptions: 1) The cluster masses grow with collision energy. 2) The rapidity space occupied by clusters depends on inelasticity and collision energy. 3) The decay of clusters of masses $M_{cl} \gg m_\pi$ is similar to the hadronization processes in e^+e^- annihilation. An account of the Monte-Carlo simulation model is given. It is shown that there is the changing of the behavior of single-diffractive cross section in the energy region $\sqrt{s} \simeq 50$–200 GeV.

The investigation has been performed at the Laboratory of Computing Techniques and Automation, JINR.

Preprint of the Joint Institute for Nuclear Research. Dubna 1988

33 коп.

Редактор Э.В.Ивашкевич.**Макет** Р.Д.Фоминой.

Подписано в печать 05.12.88.
Формат 60x90/16. Офсетная печать. Уч.-изд.листов 2,2.
Тираж 490. **Заказ** 41368.
Издательский отдел Объединенного института ядерных исследований.
Дубна Московской области.